



Enhanced thermoelectric properties of Nb-doped SrTiO₃ polycrystalline ceramic by titanate nanotube addition

Ning Wang*, Hongcai He, Xiao Li, Li Han, Chunqiu Zhang

State Key Lab of Electronic Thin Films & Integrated Devices, University of Electronic Science and Technology of China, Chengdu 610054, PR China

ARTICLE INFO

Article history:

Received 23 April 2010

Received in revised form 22 June 2010

Accepted 30 June 2010

Available online 7 July 2010

Keywords:

Ceramics
Oxide materials
Thermoelectric
Strontium titanate

ABSTRACT

The effects of titanate nanotube (TNT) addition on the thermoelectric properties of Nb-doped SrTiO₃ polycrystalline ceramic are discussed. Nb-doped SrTiO₃ ceramic composite with TNT addition was fabricated by the pressure-less sintering method in an Ar atmosphere. TNT addition significantly enhanced the ratio of the electrical conductivity to thermal conductivity. Meanwhile, the Seebeck coefficient was almost independent of TNT addition, thus, enhancing the dimensionless thermoelectric figure of merit (ZT-value). The sample with TNT addition (2 vol%) gave the maximum ZT-value of 0.14 at 900 K. The reason for the enhanced thermoelectric properties by TNT addition was also investigated.

© 2010 Elsevier B.V. All rights reserved.

1. Introduction

In order to improve the performances of thermoelectric materials, thermal conductivity should be decreased, and electrical conductivity should be increased: the two requirements can go together by using some types of nanocomposites. Thermoelectric bulk materials with nanostructured constituents have been proposed to be promising materials with high thermoelectric performances [1]. Recently, a variety of thermoelectric bulk nanocomposite materials with higher thermoelectric properties than bulk materials have been prepared. Zhang et al. prepared Ag_xSb_{2-x}Te_{3-x} thermoelectric materials with nanostructured Ag₂Te embedded in the AgSbTe₂ matrix by in situ precipitation method, and the maximum dimensionless thermoelectric figure of merit (ZT-value) of 1.53 was obtained at 500 K [2]. Sun et al. fabricated Zn₄Sb₃/Bi_{0.5}Sb_{1.5}Te nanocomposite with Zn₄Sb₃ nanoparticles using a method of vacuum melting and ball milling, followed by a vacuum hot-pressing, and the maximum ZT-value reached 0.60 at 300 K [3]. Ahn et al. prepared PbTe/CdTe thermoelectric bulk alloys with CdTe nanocrystals by melt technique, and the obtained maximum ZT-value was 1.2 at 723 K [4]. Fan et al. fabricated Bi_{0.4}Sb_{1.6}Te₃ nanocomposites through mixing nanostructured Bi_{0.4}Sb_{1.6}Te₃ particles with micron-sized particles,

and a maximum ZT-value of 1.8 at 316 K was obtained [5]. Xie et al. prepared Bi_{0.52}Sb_{1.48}Te₃ bulk materials with nanostructure by combining melt spinning technique with spark plasma sintering, and the maximum ZT-value reached 1.56 at 300 K [6]. Li et al. fabricated skutterudites In_xCe_yCo₄Sb₁₂ with in situ forming nanostructured InSb phase by a melt-quench-anneal-spark plasma sintering method, and the maximum ZT-value of 1.43 was obtained at 800 K [7]. Lan et al. prepared bulk nanograined bismuth antimony telluride by a ball milling and hot-press method, and the maximum ZT-value reached 1.4 at 373 K [8].

Very recently, we prepared Nb-doped SrTiO₃ composites with nanostructured yttria stabilized zirconia addition and mesoporous silica addition by the pressure-less sintering method [9,10]. We found they could obviously enhance the electrical conductivity by promoting densification, and then enhanced the ZT-value, which strongly triggered our interest to further investigate other effective nanosized additions to enhance the thermoelectric properties of Nb-doped SrTiO₃.

Herein, we used titanate nanotube (TNT) as the nanosized addition, and investigated its effects on the thermoelectric properties of Nb-doped SrTiO₃ ceramic.

2. Experimental procedures

First, single-phase Nb-doped SrTiO₃ (Sr(Ti_{0.85}Nb_{0.15})O₃, Nb-STO) powder was prepared by a solid-state reaction of SrCO₃, TiO₂, and Nb₂O₅ powders at 1400 °C for 4 h in an Ar atmosphere. Second, homemade titanate nanotubes (TNT) (8–10 nm of outer diameter and 3–5 nm of inner diameter) prepared according to Ref. [11] were homogeneously mixed into Nb-doped SrTiO₃ powder by hand-milling for 1 h. Furthermore, composite pellets were prepared under a pressure of 20 MPa. Finally, Nb-doped SrTiO₃ ceramic samples without TNT and with TNT addition of 2 vol% were fabricated by the pressure-less sintering method at 1500 °C for 3 h in an Ar

* Corresponding author at: State Key Lab of Electronic Thin Films & Integrated Devices, University of Electronic Science and Technology of China, Jianshe North Road, Block 2, No. 4, Chengdu, Sichuan 610054, PR China. Tel.: +86 28 8320 3807; fax: +86 28 8320 2569.

E-mail address: wangninguestc@gmail.com (N. Wang).

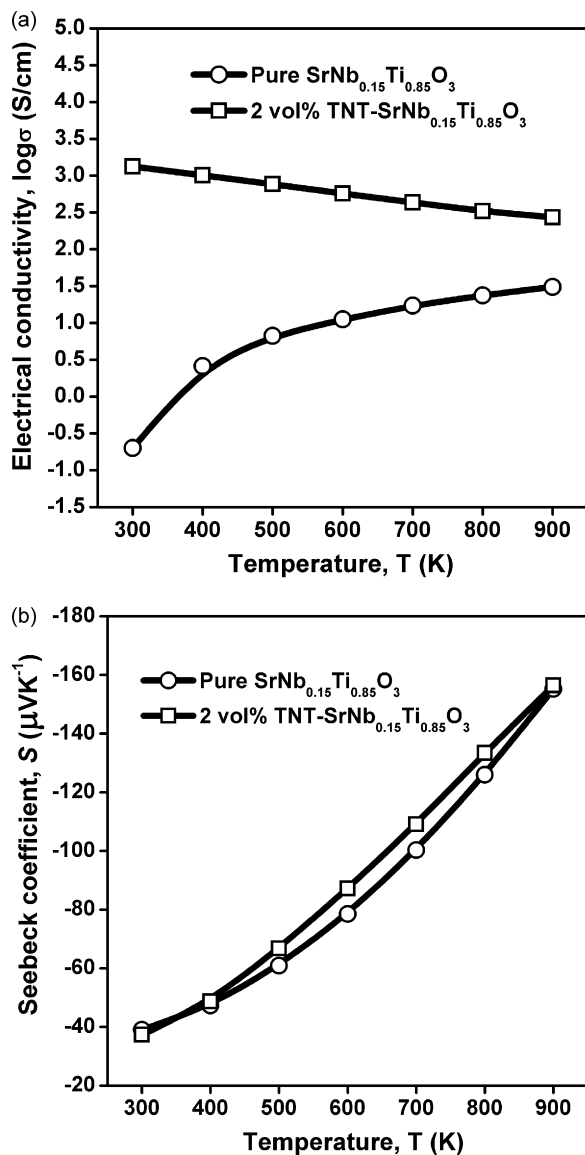


Fig. 1. Temperature dependent electric transport properties of TNT/Nb-STO composites: (a) electrical conductivity and (b) Seebeck coefficient.

atmosphere. During sintering process, the samples were kept in a graphite crucible.

The crystalline phases were determined by powder X-ray diffraction (XRD, RINT-2100, Rigaku Corporation). The morphologies of the specimens were observed by a scanning electron microscope (SEM, S-3000N, Hitachi Corporation). The thermoelectric properties, including the Seebeck coefficient and electrical conductivity, were measured at 300–900 K in an Ar atmosphere using an automatic thermoelectric measuring apparatus (RZ-2001K, Ozawa Scientific Corporation). The thermal conductivity (κ) was calculated from the thermal diffusivity (β), specific heat capacity (C_p), and density (ρ) using the following equation, $\kappa = \rho C_p \beta$. The thermal diffusivity was measured by the common laser flash method (TC-9000 V, ULVAC-RIKO Corporation). The specific heat capacity was measured by a differential scanning calorimeter system (DSC-2910, TA Instruments Corporation).

3. Results and discussion

Fig. 1 shows the temperature dependent electric transport properties of TNT/Nb-STO composites, namely, electrical conductivity (σ) and Seebeck coefficient (S). Significantly, TNT addition increased the electrical conductivity (Fig. 1(a)). Meanwhile, Seebeck coefficient was subjected to a very small impact by TNT addition (Fig. 1(b)).

Fig. 2 shows the temperature dependent measured thermal conductivity of Nb-STO ceramics with and without TNT addition. On

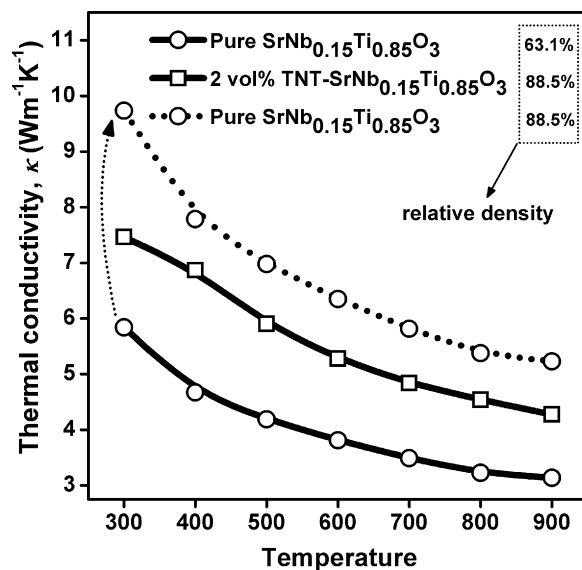


Fig. 2. Temperature dependent measured (solid line) and calculated (dotted line) thermal conductivities of TNT/Nb-STO composites.

the surface, it seemed that the thermal conductivity was increased by TNT addition. However, the relative density of these two samples drastically differed. Hence, the measured thermal conductivity does not accurately reflect the effect of TNT addition. To exclude the effect of porosity, the thermal conductivity of pure Nb-STO sample with the same relative density to the TNT/Nb-STO composite was calculated using Klemens' equation [12]:

$$\frac{\kappa_1}{\kappa_0} = 1 - \frac{4\varphi_1}{3} \quad (1)$$

$$\frac{\kappa_2}{\kappa_0} = 1 - \frac{4\varphi_2}{3} \quad (2)$$

where κ_1 and κ_2 are the thermal conductivities of the samples with different porosities (φ_1 and φ_2), and κ_0 is the thermal conductivity of the fully dense sample. Further, we can obtain the following relationship:

$$\frac{\kappa_1}{\kappa_2} = \frac{1 - 4\varphi_1/3}{1 - 4\varphi_2/3} \quad (3)$$

According to Eq. (3), the thermal conductivity of pure Nb-STO sample with the same relative density to the TNT/Nb-STO composite, 88.5%, was obtained, shown by dotted lines in Fig. 2. It was found that TNT addition could indeed reduce the thermal conductivity of Nb-STO polycrystalline ceramics when the relative density was the same.

The thermoelectric power factor $S^2\sigma$ and dimensionless figure of merit ZT of the composite are shown in Fig. 3. The power factor was increased by more than eightfold as compared with the sample without TNT addition (Fig. 3(a)), which was mainly beneficial from the significantly increased electrical conductivity. Owing to the increase in the power factor was much more than the increase in the thermal conductivity, the ZT -value was enhanced obviously (Fig. 3(b)). The maximum ZT -value, 0.14, was obtained at 900 K.

Fig. 4(a) shows the XRD pattern of the sample with TNT addition of 2 vol%. The TNT content was too low, thus only diffraction peaks from STO could be detected. To verify whether TNT addition reacted with STO at high temperatures, we increased the TNT content to 30 vol% (Fig. 4(b)), and a new phase, rhombohedral Ti_3C_5 ($a = b = 0.6115 \text{ nm}$, $c = 1.490 \text{ nm}$, JCPDS72-2496), was formed, strongly suggesting that TNT addition also reacted with STO to form titanium carbide in the sample with TNT content of 2 vol%, even

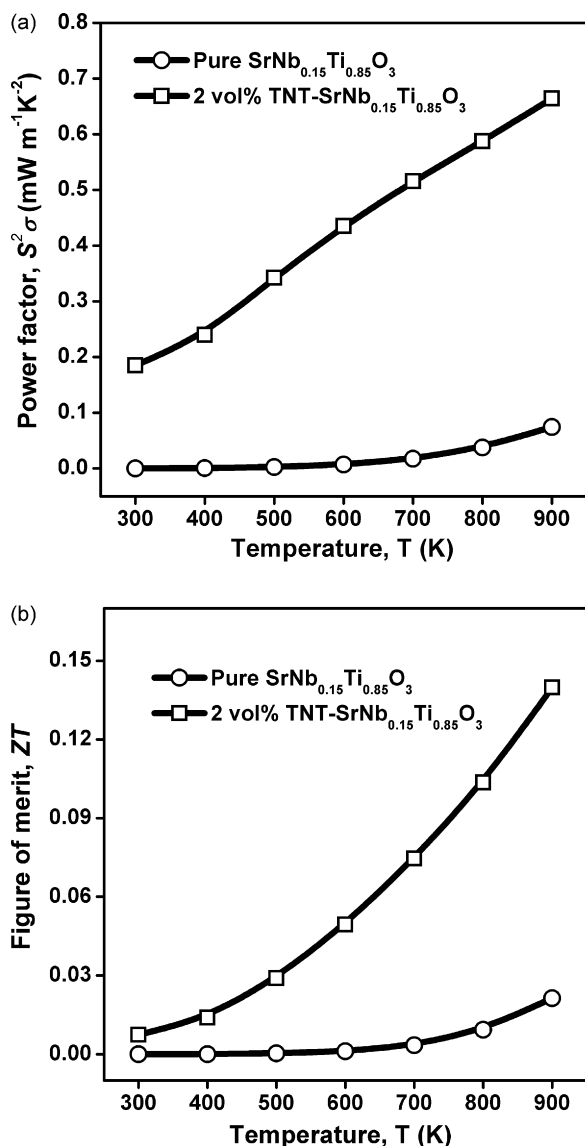


Fig. 3. Temperature dependent thermoelectric power factor $S^2\sigma$ (a) and dimensionless figure of merit ZT (b) of TNT/Nb-STO composites.

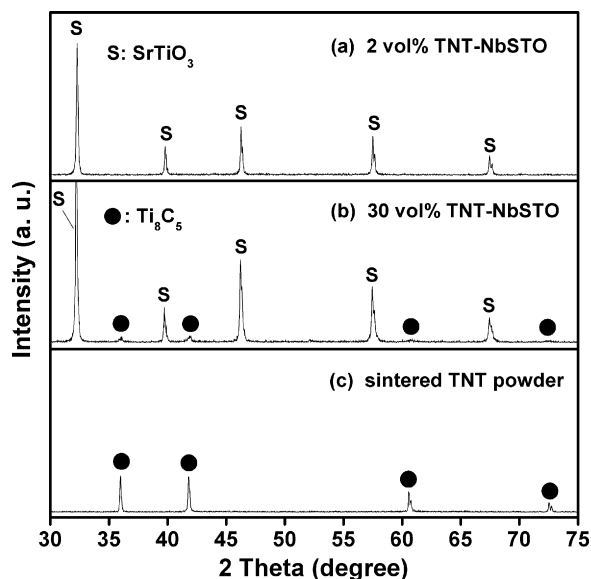


Fig. 4. XRD patterns of TNT/Nb-STO composite with various TNT contents: (a) 2 vol%; (b) 30 vol%, and pure TNT powder obtained by sintering at 1500 °C for 3 h in an Ar atmosphere (c).

though it was not detected in the XRD patterns. The carbon element was from the graphite crucible.

Fig. 5 shows scanning electron micrographs (SEM) of Nb-STO ceramics with and without TNT addition. It was found that TNT addition promoted the grain growth of Nb-STO markedly. As with SrTiO_3 ceramic, generally, when the sintering temperature was over than 1250 °C, the volume diffusion was the main sintering mechanism [13]. Nb-STO composite with TNT addition was Ti-rich and Ti excess could create Sr and O vacancies and therefore promoted volume diffusion. Grain growth of Nb-STO reduced interface scattering of the electrons, enhanced carrier mobility [10], and further increased the electrical conductivity. In addition, the generated titanium carbide had very high electrical conductivity, $>10^4 \text{ S cm}^{-1}$ at room temperature [14], which could also contribute to the increased electrical conductivity. We found that there were lots of pores distributed homogeneously in the Nb-STO bulk ceramic (Fig. 5(b)). Even though the possible reason for the formation of homogeneously distributed pores inner the grain was not clear, these pores located homogeneously in the

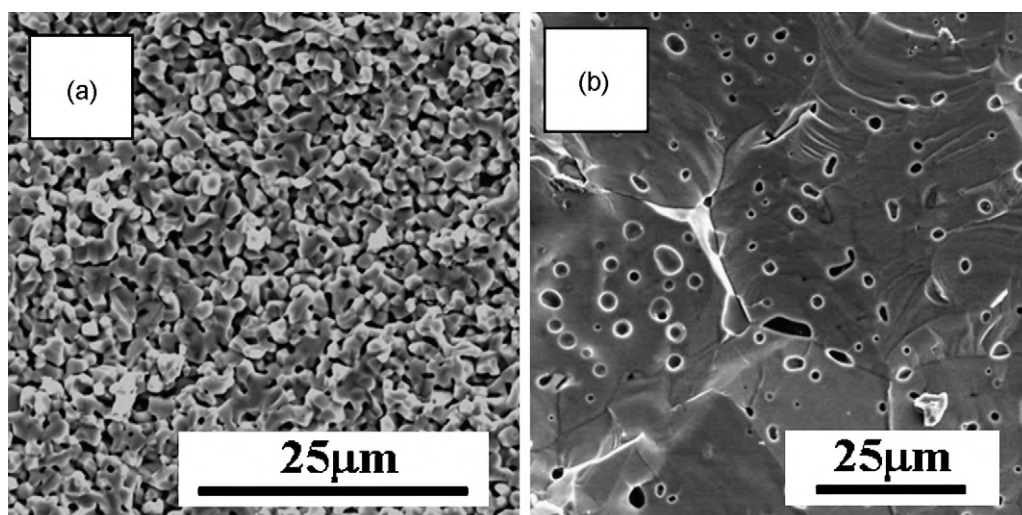


Fig. 5. SEM micrographs of TNT/Nb-STO composites with various TNT contents: (a) 0 vol% and (b) 2 vol%.

Nb-STO bulk ceramic could scatter phonons effectively, which might be the main reason for the reduced thermal conductivity of TNT/Nb-STO composite with the same relative density to pure Nb-STO ceramic, even though the generated titanium carbide had very high thermal conductivity, $>15 \text{ Wm}^{-1} \text{ K}^{-1}$ at 50°C [14].

For degenerate semiconductors for which a parabolic band and energy-independent scattering approximation can be assumed [15], the Seebeck coefficient (S) can be given by the following equation:

$$S = \frac{8\pi^2 k_B^2}{3eh^2} m^* T \left(\frac{\pi}{3n} \right)^{2/3} \quad (4)$$

where k_B , h , m^* , and n are Boltzmann constant, Planck constant, the effective mass of the carriers, and the carrier concentration, respectively. Eq. (4) indicated the Seebeck coefficient strongly depended on carrier concentration. When the addition could not react with Nb-STO, carrier concentration would not be affected [10], which was the main reason for the independence of the Seebeck coefficient on TNT addition.

4. Conclusions

Titanate nanotube (TNT) addition significantly enhanced the ZT-value of Nb-STO bulk ceramic, and the sample with TNT addition (2 vol%) gave the maximum ZT-value of 0.14 at 900 K. The obviously increased electrical conductivity produced the enhanced ZT-value, even although the measured thermal conductivity increased. Enhancement of the electrical conductivity was mainly caused by promoted grain growth and newly generated titanium carbide with higher electrical conductivity. Seebeck coefficient was almost independent of TNT addition, which was mainly because that the carrier concentration had not been affected by TNT addition.

Acknowledgments

The authors are grateful to International Cooperation MOST-JST Program Fund (No. 2010DFA61410), Western Light Project of Chinese Academy of Sciences (No. LHXZ200902), National Natural Science Foundation of China (No. 50802013), Research Fund for Doctoral Program of Higher Education (No. 200806141019), and Open Fund of State Key Lab of New Ceramics & Fine Processing (Tsinghua University).

References

- [1] M.S. Dresselhaus, G. Chen, M.Y. Tang, R. Yang, H. Lee, D. Wang, Z. Ren, J.P. Fleurial, P. Gogna, *Adv. Mater.* 19 (2007) 1043–1053.
- [2] S.N. Zhang, T.J. Zhu, S.H. Yang, C. Yu, X.B. Zhao, *J. Alloys Compd.* 499 (2010) 215–220.
- [3] J.H. Sun, X.Y. Qin, H.X. Xin, D. Li, L. Pan, C.J. Song, J. Zhang, R.R. Sun, Q.Q. Wang, Y.F. Liu, *J. Alloys Compd.* 500 (2010) 215–219.
- [4] K. Ahn, M.K. Han, J. He, J. Androulakis, S. Ballikaya, C. Uher, V.P. Dravid, M.G. Kanatzidis, *J. Am. Chem. Soc.* 132 (2010) 5227–5235.
- [5] S. Fan, J. Zhao, J. Guo, Q. Yan, J. Ma, H.H. Hng, *Appl. Phys. Lett.* 96 (2010) 182104.
- [6] W. Xie, X. Tang, Y. Yan, Q. Zhang, T.M. Tritt, *Appl. Phys. Lett.* 94 (2009) 102111.
- [7] H. Li, X. Tang, Q. Zhang, C. Uher, *Appl. Phys. Lett.* 94 (2009) 102114.
- [8] Y. Lan, B. Poudel, Y. Ma, D. Wang, M.S. Dresselhaus, G. Chen, Z. Ren, *Nano Lett.* 9 (2009) 1419–1422.
- [9] N. Wang, L. Han, H. He, Y. Ba, K. Koumoto, *J. Alloys Compd.* 497 (2010) 308–311.
- [10] N. Wang, L. Han, Y. Ba, Y. Wang, C. Wan, K. Fujinami, K. Koumoto, *J. Electron. Mater.* (2010), doi:10.1007/s11664-010-1144-1.
- [11] N. Wang, H. Lin, J. Li, L. Zhang, C. Lin, X. Li, *J. Am. Ceram. Soc.* 89 (2006) 3564–3566.
- [12] P.G. Klemens, *High Temp. High Press* 45 (4) (1973) 574–588.
- [13] M. Bäurer, H. Kung, M.J. Hoffmann, *J. Am. Ceram. Soc.* 92 (2009) 601–606.
- [14] W. Lengauer, S. Binder, K. Ainger, P. Ettmayer, A. Gillou, J. Debuigne, G. Groboth, *J. Alloys Compd.* 217 (1995) 137–147.
- [15] M. Cutler, J.F. Leavy, R.L. Fitzpatrick, *Phys. Rev.* 133 (1964) A1143–A1152.